Journal of Human Genetics
https://doi.org/10.1038/s10038-019-0641-1

ARTICLE

Entire *FGF12* duplication by complex chromosomal rearrangements associated with West syndrome

Yoichiro Oda[1] · Yuri Uchiyama[2,3] · Ai Motomura[1] · Atsushi Fujita[2] · Yoshiteru Azuma[2] · Yutaka Harita[4] · Takeshi Mizuguchi[2] · Kumiko Yanagi[5] · Hiroko Ogata[6] · Kenichiro Hata[6] · Tadashi Kaname[5] · Yoichi Matsubara[7] · Keiko Wakui[8] · Naomichi Matsumoto[2]

Received: 23 April 2019 / Revised: 23 June 2019 / Accepted: 26 June 2019

Abstract

Complex rearrangements of chromosomes 3 and 9 were found in a patient presenting with severe epilepsy, developmental delay, dysmorphic facial features, and skeletal abnormalities. Molecular cytogenetic analysis revealed 46,XX.ish der(9)(3qter→3q28::9p21.1→9p22.3::9p22.3→9qter)(RP11–368G14+,RP11–299O8−,RP11–905L2++,RP11–775E6++). Her dysmorphic features are consistent with 3q29 microduplication syndrome and inv dup del(9p). Trio-based WES of the patient revealed no pathogenic single nucleotide variants causing epilepsy, but confirmed a 3q28q29 duplication involving *FGF12*, which encodes fibroblast growth factor 12. FGF12 positively regulates the activity of voltage-gated sodium channels. Recently, only one recurrent gain-of-function variant [NM_021032.4:c.341G>A:p.(Arg114His)] in *FGF12* was found in a total of 10 patients with severe early-onset epilepsy. We propose that the patient's entire *FGF12* duplication may be analogous to the gain-of-function variant in *FGF12* in the epileptic phenotype of this patient.

Introduction

Fibroblast growth factor 12 encoded by the *FGF12* gene, is an accessory protein which binds to the C-terminal of the alpha-subunit of fast sodium channels associated with voltage-dependent inactivation [1]. Siekierska et al. recently reported a recurrent pathogenic variant of *FGF12* [NM_021032.4:c.341G>A:p.(Arg114His)], which causes early-onset epileptic encephalopathies with cerebellar atrophy [2], To date, a total of 10 patients with the identical *FGF12* variant (c.341G>A) have been reported [2–6]. Takeguchi et al. suggested that the phenotypic features of this *FGF12* recurrent variant include severe epileptic spasms with/without the brain abnormality characterized by cerebral atrophy [6].

In this study, we encountered a 14-year-old Japanese girl with complex chromosomal rearrangements. We present a detailed clinical evaluation together with intensive genomic analysis, and discuss new evidence for the etiology of epileptic encephalopathy.

These authors contributed equally: Yoichiro Oda, Yuri Uchiyama

Supplementary information The online version of this article (https://doi.org/10.1038/s10038-019-0641-1) contains supplementary material, which is available to authorized users.

✉ Naomichi Matsumoto
naomat@yokohama-cu.ac.jp

[1] Department of Pediatrics, Chigasaki Municipal Hospital, Chigasaki, Japan

[2] Department of Human Genetics, Yokohama City University Graduate School of Medicine, Yokohama, Japan

[3] Department of Oncology, Yokohama City University Graduate School of Medicine, Yokohama, Japan

[4] Department of Pediatrics, Graduate School of Medicine, The University of Tokyo, Tokyo, Japan

[5] Department of Genome Medicine, National Center for Child Health and Development, Tokyo, Japan

[6] Department of Maternal-Fetal Biology, National Research Institute for Child Health and Development, Tokyo, Japan

[7] National Research Institute for Child Health and Development, Tokyo, Japan

[8] Department of Medical Genetics, Shinshu University School of Medicine, Matsumoto, Japan

Published online: 16 July 2019

Material and methods

Patient

The 14-year-old female patient (II-1) and her parents (I-1 and I-2) participated in Initiative on Rare and Undiagnosed Diseases (IRUD) in Japan. Written informed consent to participate in this study was obtained from the patient and her parents. This study was approved by Institutional Review Boards of Yokohama City University Graduate School of Medicine, National Center for Child Health and Development and Tokyo University Graduate School of Medicine, and Shinshu University School of Medicine.

Genetic analysis

Whole exome sequencing

Trio-based whole exome sequencing (WES) was performed for the patient and her parents. Genomic DNA was extracted from peripheral blood leukocytes using a standard method, captured by the SureSelect Human All Exon v6 (Agilent Technologies, Santa Clara, CA, USA), and sequenced on an Illumina HiSeq 2500 system (Illumina, San Diego, CA, USA) using 101-bp paired-end reads. Exome data was processed as previously described [7, 8]. The mean whole exome sequencing read depth in the RefSeq protein-coding regions was 70.38×, 73.29×, and 70.41× for the proband, her father and her mother, respectively. There was at least 94.4% coverage of the target regions with 20 reads or more in all of them. To identify causal variants for neurodevelopmental disorders, variants were excluded that were either synonymous, registered in our in-house whole exome database of 575 Japanese control individuals, or in the NHLBI Exome Sequencing Project (http://evs.gs.washington.edu/EVS/), Human Genetic Variation Database (http://www.genome.med.kyoto-u.ac.jp/SnpDB/) [9], Exome Aggregation Consortium (http://exac.broadinstitute.org/), or Tohoku Medical Megabank Organization (http://www.megabank.tohoku.ac.jp/english/) databases. We evaluated the remaining variants under the assumption of autosomal dominant, recessive, and X-linked dominant disease, with particular focus on rare variants in known genes for neurodevelopmental disorders. Copy number variations (CNVs) were detected from the WES data as previously described [10, 11]. Two algorithms were used: the eXome-Hidden Markov Model (XHMM) and Nord's method [12, 13]. In brief, XHMM detects CNVs by analyzing normalized raw exome read depth data with principal-component analysis (PCA) of the complete coding regions. Nord's method was performed using genes mapped around the region identified by XHMM.

Quantitative PCR (qPCR)

In order to confirm the CNVs which were detected from the WES data using XHMM and Nord's method, qPCR was performed using the Rotor-Gene Q real-time PCR cycler (Qiagen, Hilden, Germany) as previously described [14, 15]. Briefly, two primer sets were designed for each CNV region. The Rotor-Gene SYBR Green PCR kit (Qiagen) was used for the current qPCR testing according to the manufacture's manual. *STXBP1* (NG_016623.1) and *FBN1* (NG_008805.2) genes were used as references. The sequences of the primers are shown in Table S1. Each qPCR reaction was performed in duplicate and relative quantification analysis was performed using the relative standard curve method.

G-banded karyotyping and multi-color FISH

G-banded karyotyping and multi-color FISH of the patient's chromosomes were performed by LSI Medience Corporation (Chiyoda-ku, Tokyo, Japan). Analysis was performed under the provision of information from the CNV analysis.

Fluorescence in situ hybridization (FISH)

Metaphase chromosomes from the patient were prepared from her peripheral blood leukocytes as previously described [14, 15]. Briefly, appropriate RPCI-11 human bacterial artificial chromosome (BAC) clones were selected from the genome database to confirm the chromosomal rearrangements related to CNVs of chromosomes 3 and 9. One hundred nanogram of each DNA from BAC clone was labeled using the nick translation kit (Abbott Molecular, Des Plaines, IL) with Green-dUTP, Orange-dUTP, or Aqua-dUTP (Enzo Life Science, Farmingdale, NY). Three probes labeled with different colors were mixed and hybridized to chromosome preparation for 24–48 h. After washing, VECTASHIELD Antifade Mounting Medium with 4′,6-diamidino-2-phenylindole (DAPI) (Vector Laboratories, Burlingame, CA) was used for counterstaining and mounting on slides. Images were captured using the Carl Zeiss Microscopy Axio imager M2 (Carl Zeiss, Oberkochen, Germany) and Carl Zeiss Microscopy Zen2 (Carl Zeiss).

Results

Clinical information

Detailed clinical features of the patient are summarized in Table 1 and Table S6. The proband (II-2) showed severe

Table 1 Clinical features of the current and reported patients with inv dup del(9)

	Current case	Recalcati et al.	Hulik et al.	Swinkles et al. case 6	Swinkles et al. case 7	
	(XX)	(XY)	(XX)	(XX)	(XX)	
9p deleted region	9p24.3p22.3	9p24.3p22.2	9p24.3p24.2	9p24.3p22.2	9p24.3p22.3	
9p duplicated region	9p22.3p21.1	9p22.2p12	9p24.2p21.3	9p22.2p13.3	9p22.3p12	Count (ratio %)
9p deletion/duplication features						
Developmental delay	+	+	+	+	+	5/5 (100)
Psychomotor retardation	+	+	+	+	+	5/5 (100)
Hypotonia	−	+	+	+	+	4/5 (80)
Hypertelorism	+	+	+	−	−	3/5 (60)
Low-set and posteriorly angulated ears	+	+	+	+	+	5/5 (100)
Skeletal malformations	+	+	−	+	−	3/5 (60)
9p deletion features						
Trigonocephaly	−	−	−	+	+	2/5 (40)
Midface hypoplasia	+	+	+	+	+/−	4/5 (80)
Up slanting palpebral fissures	−	−	−	−	+	1/5 (20)
Short palpebral fissures	−	−	−	+	+	2/5 (40)
Anteverted nostrils	+	−	−	+	+	3/5 (60)
Long philtrum	+	+	+	+	+/−	4/5 (80)
Thin upper lip	+	+	+	+	+	5/5 (100)
Micrognathia	−	−	+	+	+	3/5 (60)
Short/broad neck	+	+	−	+	−	3/5 (60)
Cardiac defects	−	+	−	+	+	3/5 (60)
Genital/gonadal disorders	−	+	−	−	−	1/5 (20)
Inguinal hernia	−	+	−	−	−	1/5 (20)
Omphalocele	−	−	−	+	−	1/5 (20)
9p duplication features						
Speech/language delay	+	+	NA	+	+	4/5 (80)
Growth retardation/ short stature	+	−	+	+	+	4/5 (80)
Microcephaly/brachycephaly	−	+	−	−	−	1/5 (20)
Deep and wide-set eyes	−	−	+	−	−	1/5 (20)
Down slanting palpebral fissures	+	+	−	−	−	2/5 (40)
Bulbous nasal tip	+	+	+	+	+	5/5 (100)
Short philtrum	−	−	−	−	−	0/5 (0)
Downturned corners of the mouth	−	−	+	−	−	1/5 (20)
Highly arched palate	+	+	−	+	+	4/5 (80)
Cleft palate/lip	−	−	+	−	−	1/5 (20)
Toes with short/dystrophic nails	−	−	+	−	−	1/5 (20)
Clinodactyly	−	−	+	−	−	1/5 (20)
Epilepsy	+	−	−	−	−	1/5 (20)

Note: This table was referred to Table 2 in the previous report by Recalcati et al. [23]

NA not available

epilepsy, hypoglycemia with hyperinsulinemia, multiple dysmorphic features, motor developmental delay, intellectual disability, and congenital hypothyroidism (Fig. 1d–g). She was born to non-consanguineous Japanese parents (I-1 and I-2) at 35 weeks of gestation with an Apgar score of 9 at 1 min and 10 at 5 min. She was admitted to the new-born intensive care unit (NICU) due to hypoglycemic convulsion, which occurred on the first day of life. After admittance to the NICU, where she received continuous administration of a glucose infusion, octreotide, and

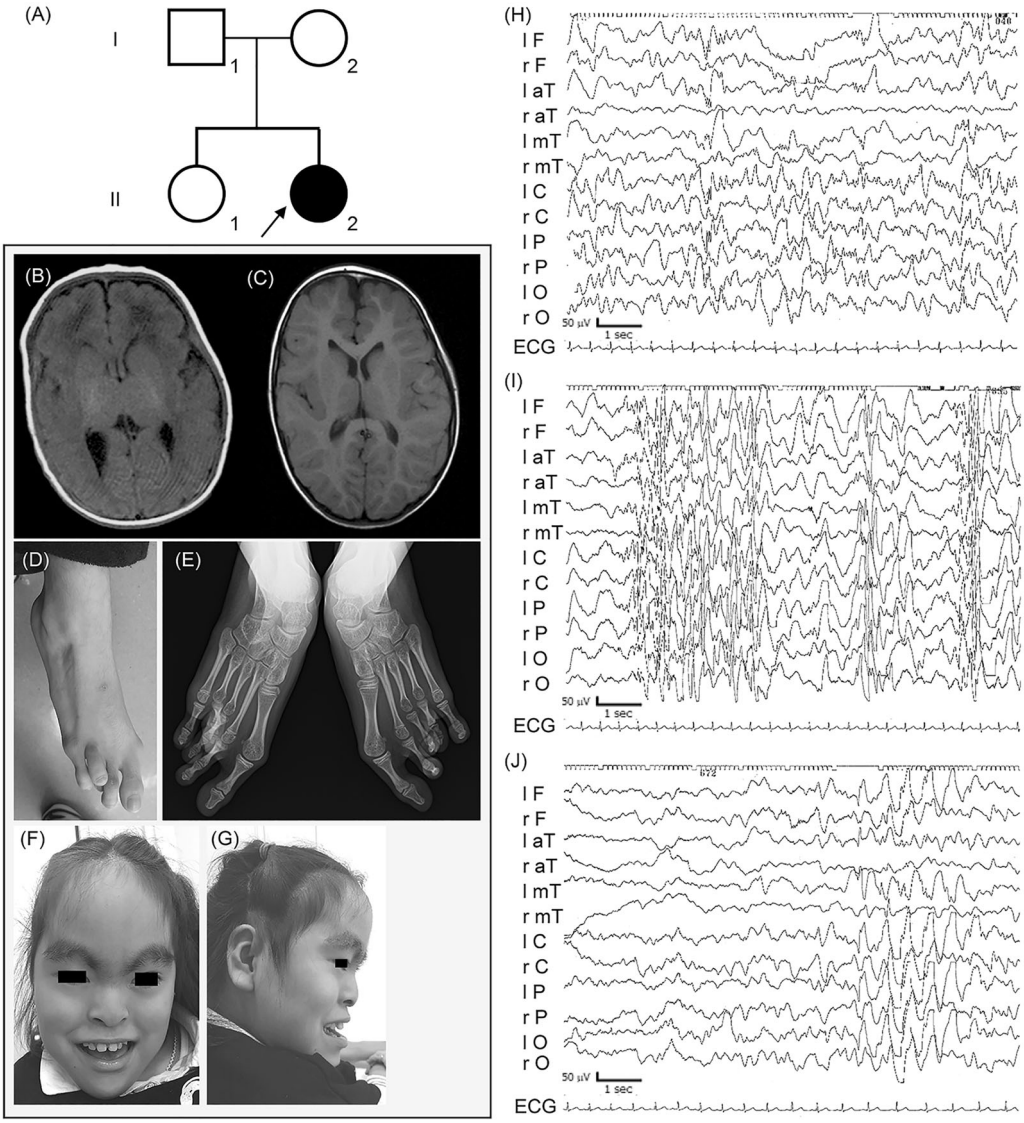

Fig. 1 Clinical presentation of the identified 3q28q29 duplications with inv dup del(9p). **a** Pedigree of the current family. The proband is indicated with arrow. **b** and **c** T1 weighted brain magnetic resonance imaging (MRI) at 41 days following birth (**b**) and at four years of age indicating mild frontal brain atrophy (**c**). **d** Picture of right foot indicating third toe overlapped by fourth toe. **e** Bilateral X-ray of feet showing short third and fourth bradymetatarsus. **f** and **g** Facial pictures of the patient indicating low-set and posteriorly angulated ears, hypertelorism, down slanting palpebral fissures, mid face hypoplasia, bullous nasal tip, anteverted nostrils, long philtrum, and thin upper lip. **h** Electroencephalogram (EEG) at 26 weeks of age showing left anteriotemporal polyspike-wave pattern. **i** Electroencephalogram (EEG) at eleven months of age showing hypsarrhythmia. **j** EEG at 12 days after the initiation of intravenous immunoglobulin therapy for epileptic spasms indicating disappearance of hypsarrhythmia

leucine-reduced milk. After intensive care with administration of continuous glucose infusion, octreotide, and leucine-reduced milk, she could keep her sufficient blood glucose level with 10 mg/kg diazoxide. Repeated abdominal ultrasonic echography revealed no morphological abnormalities of the pancreas. In the neonatal period, she exhibited hyperbilirubinemia, which required phototherapy and exchange transfusion; and congenital central hypothyroidism, which was treated with levothyroxine (LT4). Magnetic resonance imaging (MRI) at the age of 4 years showed normal pituitary and laboratory data that did not suggest any hypopituitarism.

Despite maintaining sufficient glucose levels, she developed paroxysmal episodes of motion arrest and staring at age six weeks. These episodes once disappeared after starting oral phenobarbital with the diagnosis of epilepsy although inter-ictal EEG was normal findings. Additional zonisamide was effective against the seizures of tonic posturing with staring at age 16 weeks. Interictal EEG at age of 26 weeks first revealed abnormal patterns such as multifocal

spike-wave and polyspike-wave (Fig. 1h). She developed epileptic spasms with clusters as dozen times per day at age 11 months with hypsarrhythmia on interictal EEG (Fig. 1i). We chose intravenous immunoglobulin therapy (IVIG) prior to adrenocorticotropic hormone because we considered the side effects to hyperglycemia and severe infection. IVIG successfully led to termination of spasms in one week, and disappearance of hypsarrhythmia was confirmed at 12th day (Fig. 1j) [16]. However, partial seizures with unconsciousness, which were resistant to multiple antiepileptic drugs, have remained. Initial MRI findings at the age of 41 days were unremarkable, but the second MRI indicated mild frontal lobe atrophy at the age of 4 years (Fig. 1b, c). She could not stand without support and could speak only two-word-sentence at the age of 14 years. Her birth length, weight, and head circumference was 47.0 cm (SD: 0.0), 2.35 kg (SD: 0.7), and 33.5 cm (SD: −0.7), respectively. At the age of 14 years, her height, weight, body mass index, and head circumference was 147.0 cm (SD: −1.82), 37.7 kg (SD: −2.18), 17.4 (percentile: 11.5), and 52.4 cm (SD: −1.99), respectively.

Identification of the current structural variation from WES data

Trio-based WES analysis did not detect any causative variants in known genes related to neurodevelopmental disorders with epilepsy. On the other hand, the large deletion and duplications at chromosome 3 and chromosome 9 were detected by XHMM (Table S2, S3 and S4). A large duplication from 3q28-q29(3qter) (7.2 Mb in size), a large deletion from 9p24.3(9pter)-p22.3 (14.2 Mb) and a large duplication of 9p22.3-p21.1 (17.4 Mb) were identified both by Nord's method and qPCR (Fig. 2a, b).

Structural rearrangements revealed by fluorescence in situ hybridization

The 24-color FISH (mFISH) indicated that the subtle segment derived from chromosome 3 had translocated to one of the distal short arms of chromosome 9 (Fig. S1A, B). However, the corresponding segment of chromosome 9 was not observed anywhere other than chromosomes 9 (Fig. 3a–d and S1A, B). Together with CNV from WES data, the patient's G-banded karyotype was considered to be 46,XX.ish der(9)(3qter→3q28::9p21.1→9p22.3::9p22.3→9qter).

To address the orientation of the CNV segments, five BACs were selected (Table S5) and three color FISH was performed using two combinations (I and II) as follows. I: RP11–466H23 (3p26, labeled orange), RP11–368G14 (3q28, yellow) and RP11–775E6 (9p21.1, aqua) (Fig. 3e); II: RP11–299O8 (9p24.3, green), RP11–905L2 (9p22.2, orange), and RP11–775E6 (9p21.1, aqua) (Fig. 3i). Combination I revealed that the segments including 3q28 and 9p21.1 were both observed on derivative chromosome 9 (der(9)) (Fig. 3e–h). Combination II also confirmed that der(9) had inverted duplication of the segment 9p22.2-p21.1, and deletion of the segment including 9p24.3, as it is called inv dup del 9p. The FISH images showed a green-orange-aqua pattern (direct orientation) on normal chromosome 9 and another aqua-orange-orange-aqua pattern on der(9) (Fig. 3i–l). These patterns were consistently observed metaphases. Summarizing these data, this patient had a complex abnormal chromosome 9 consisting of unbalanced translocation between chromosome 3 and 9 with inv dup del (9p). The current chromosomal abnormalities are described as follows: 46,XX.ish der(9)(3qter→3q28::9p21.1→9p22.3::9p22.3→9qter)(RP11–368G14+,RP11–299O8−, RP11–905L2++,RP11–775E6++). We could not confirm whether our patient's rearrangements occurred de novo as the parents did not wish for their chromosomes to be analyzed.

Discussion

In this study, we encountered a 14-year-old Japanese patient with severe epilepsy, developmental delay, dysmorphic facial features, and skeletal abnormalities. We performed trio-based WES and found that the patient had the complex chromosomal rearrangements with entire *FGF12* duplication. Considering her chromosomal rearrangements, she has both 9p deletion and the 3q28q29 microduplication syndromes. The common phenotypic features observed in both typical 9p deletion syndrome and 3q29 microduplication syndrome are multiple dysmorphisms, mild to moderate psychiatric disabilities and/or delay (Table 1, S6 and S7). In the following sections, we will argue that our clinical evaluation and intensive genomic analysis suggest that the patient's epileptic encephalopathy may be caused by the gain-of-function in *FGF12* due to its duplication.

Confirming inv dup del(9p) in the current patient, clinical features were compared with those of four previously reported patients with inv dup del(9p) (Table 1) [17–20]. Common clinical features are developmental delay (5/5, 100%), psychomotor retardation (5/5, 100%) and speech/language delay (4/5, 80%) [21–23]. Head and neck dismorphologies described by Recalcati et al. are also observed in our patient (Table 1) [23].

Our patient developed neonatal-onset epilepsy followed by West syndrome, which are one of the common types of epileptic encephalopathy. However, this contrasts with the patients with 9p deletion syndrome who were previously reported [21–24]. On the other hand, the phenotypic features of 3q29 duplication syndrome (MIM611936) is heterogeneous (Table S6) [17, 18, 20, 25].

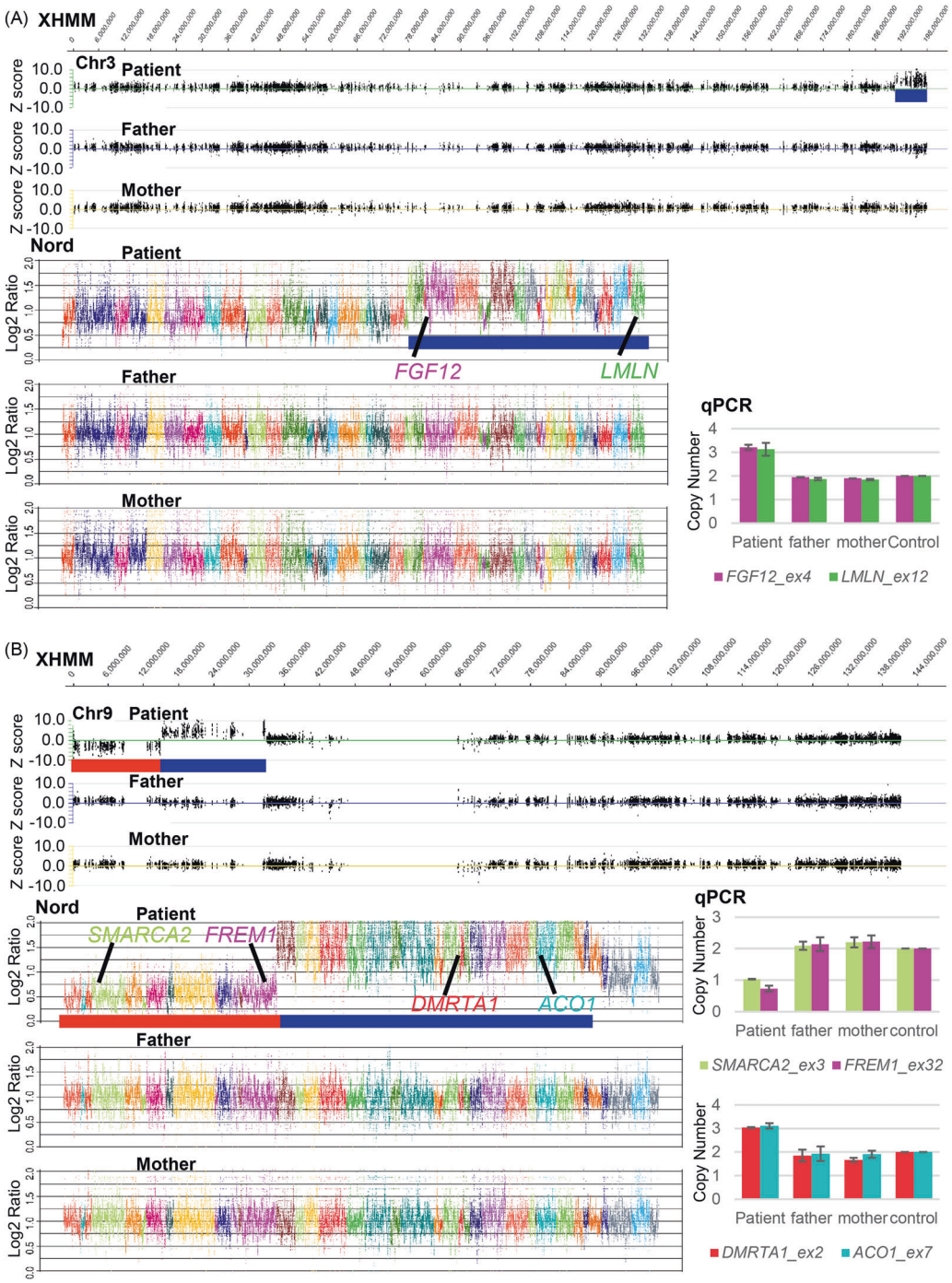

Fig. 2 Copy number changes in this patient. Copy number changes in chromosomes 3 (**a**) and 9 (**b**) based on WES data. Results from XHMM are described in the upper portion and results from Nord's method are in the lower portion. The qPCR results are shown in lower right. The total number of genes located at the duplication of 3q28q29, the deletion of 9p24.3p22.3 and the duplication of 9p22.3p21.1 are 78, 53 and 73, respectively (the lists are shown in Table S2–S4). As for XHMM, *X*-axis shows the genomic position and *Y*-axis indicates the *Z* score of each target probe. For Nord's method, 14 to 25 genes are selected, mapped around CNVs (data not shown). The *X*-axis shows arrays of targeted genes with different colors based on their proportional physical length and the *Y*-axis shows log2 ratios for each targeted base in the tested genes. In each method, blue and dark orange thick bars represent copy number gain and loss, respectively. We detected a 7.2-Mb deletion at 3q28q29, 14.2-Mb deletion at 9p24.3p22.3 and 17.4-Mb duplication at 9p22.3–9p21.1. For qPCR, *X*-axis shows respective samples, and Y-axis shows the relative copy number. Targeted genes for qPCR are shown below the bar graphs. A normal female control and family members were used reference for qPCR

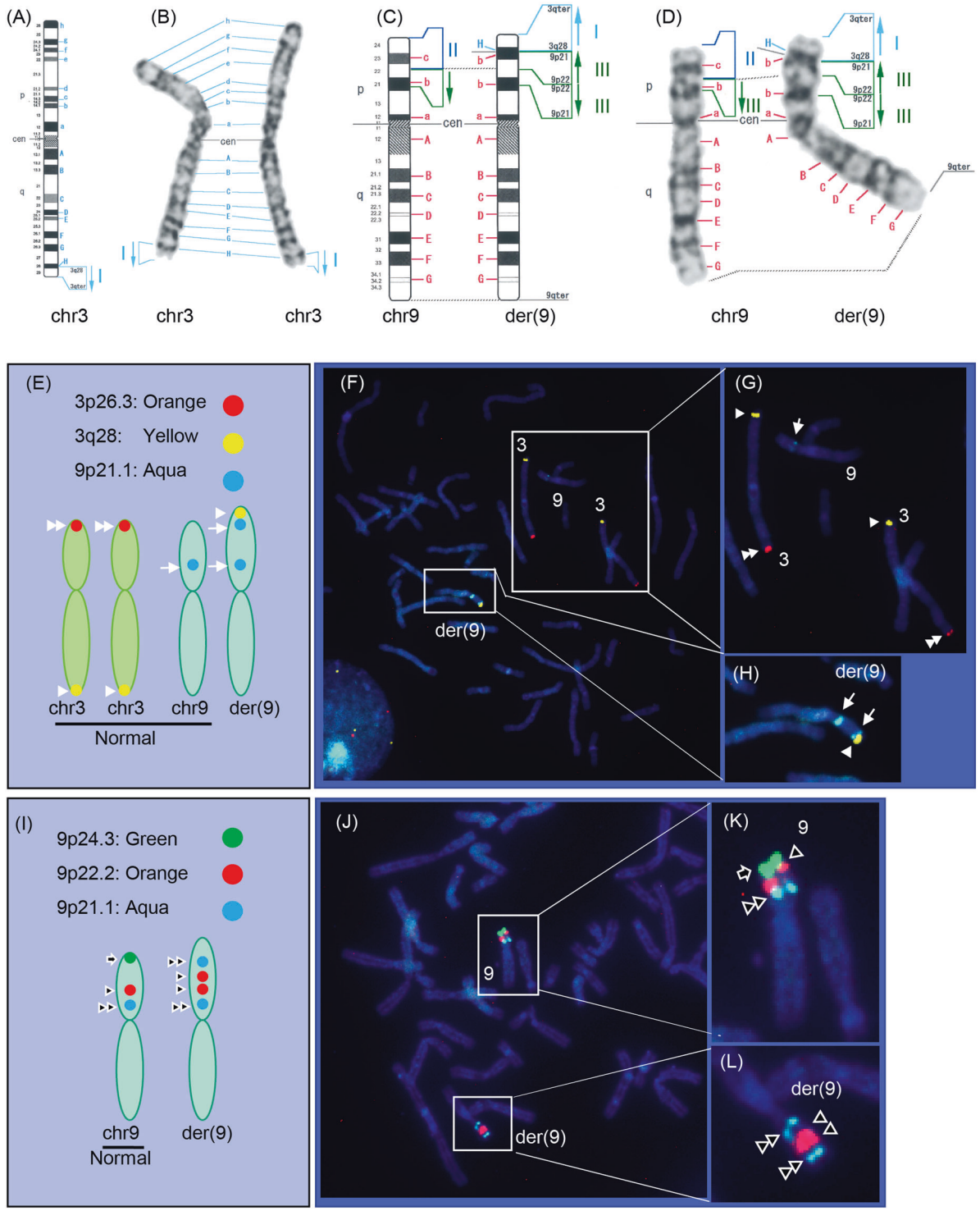

Notably, only two cases with 3q29 duplication syndrome (2/15, 13.3%) had epilepsy, while the other 13 and two cases registered in DECIPHER did not displayed no evidence of this condition (Table S6 and S7) [17–20, 25]. In fact, 3q29 duplication syndrome which has been previously described across three generations showed a mild phenotype with no epilepsy [25]. The 3q28 duplication in the current patient involved *FGF12*, which encodes fibroblast growth factor 12 (OMIM 601513) (Fig. 4). After careful evaluation of genes involved in 9p24.3p22.3 deletion, 9p22.3p22.1 duplication and 3q28ter duplication, *FGF12* only remained as a strong candidate for severe

◀ **Fig. 3** G-banded karyotyping and three-color metaphase FISH delineating inv dup del(9p). The presentation of g-banded chromosomes 3, 9, and der(9). **a**–**d** Chromosomal segments of 3q28→3qter, 9pter→p22 and 9p22 to 9p21 are indicated by I, II, and III, respectively, together with an arrow depicting the direction. **e** Schematic representation of the BAC probe mix I: 3p26.3 (RP11–466H23: orange, white doubled arrowheads), 3q28 (RP11–368G14: green, as represented in yellow, depicted by white arrowheads) and 9p21.1 (RP11–775E6: aqua, represented in blue-green, depicted by white arrow). FISH results using these BACs are shown in **f**–**h**. **f** Metaphase FISH result from the patient. Duplicated 9p21.1 (aqua) with 3q28 (yellow) on derivative chromosome 9, two normal depictions of chromosome 3 similarly signaled with 3p26.3 (orange) and 3q28 (green) and one normal chromosome 9 with 9p21.1 (blue-green). Close up views of normal chromosomes 3 and one chromosome 9 (**g**) and one derivative chromosome 9 (**h**). **i** Schematic presentation of BAC probe mix II: 9p24.3 (RP11–299O8: green, doubled black arrowheads with white outline), 9p22.2 (RP11–905L2: orange, filled black arrowheads with white outline), and 9p21.2 (RP11–775E6: aqua, filled black arrows with white outline). FISH result using these BACs are shown in **j**–**l**. **j** Metaphase FISH in the patient. Normal chromosome 9 is seen with signals of 9p24.3 (green), 9p22.2 (orange) and 9p21.1 (aqua) from 9pter to centromere. The derivative chromosome 9 with duplicated RP11–775E6 signals (aqua) between duplicated RP11–905L2 (orange). Close up views of chromosome 9 (**k**) and derivative chromosome 9 (**l**)

early-onset epileptic encephalopathy (please see Supplementary information, and Tables S8 and S9). The identical missense variant (NM_021032.4:c.341G>A:p.Arg114His) [2–6, 26, 27] and the entire *FGF12* duplication in the current both may likely be gain-of-function changes.

In our patient, despite of trio-based WES analysis and intensive chromosomal analysis, no causative variants were found which explain her congenital hypoglycemia with hyperinsulinemia and congenital central hypothyroidism [28–30]. The first and second MRI studies suggested that hypoglycemic encephalopathy was unlikely. Resistance to multiple antiepileptic drugs in controlling her epilepsy strongly indicates that it has a monogenic origin. Therefore, *FGF12* duplication, which is possibly analogous to the gain-of-function *FGF12* variant, may be the cause for her epilepsy.

In conclusion, we found a patient having 9p deletion and 3q29 microduplication syndromes together with entire *FGF12* duplication. We propose *FGF12* duplication could be similarly epileptogenic to the identical *FGF12* variant repeatedly found.

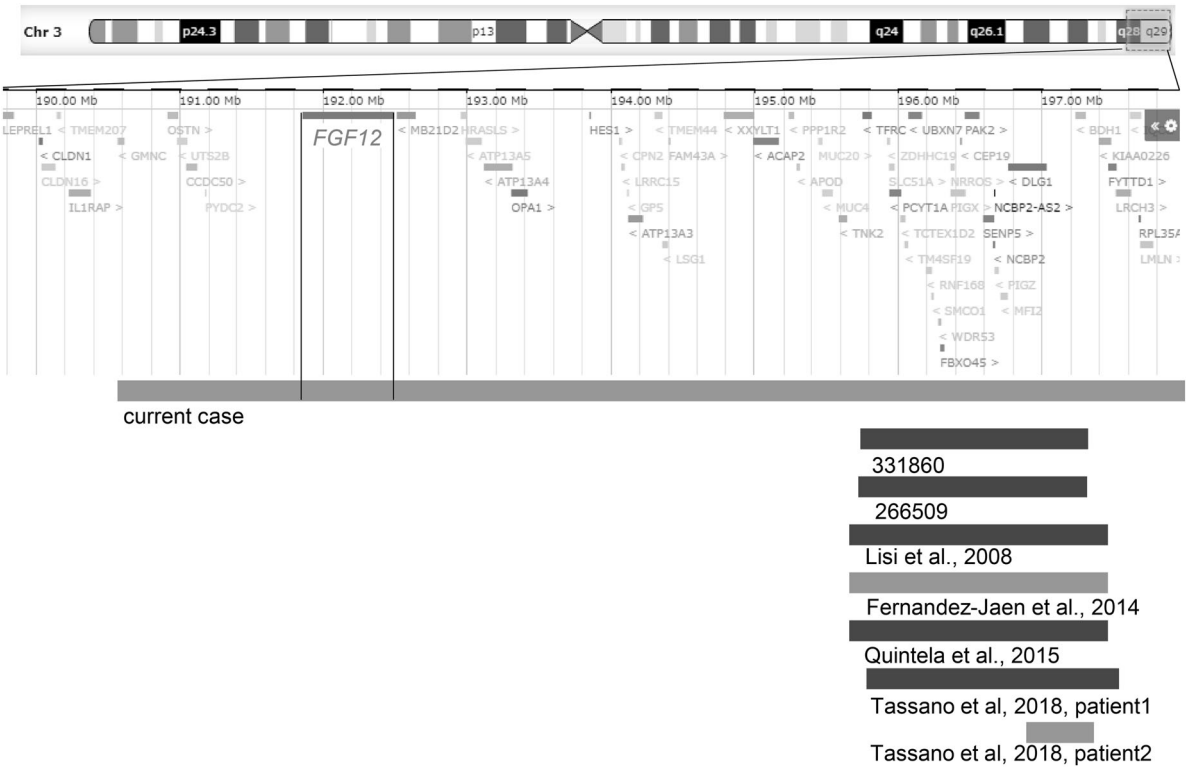

Fig. 4 3q28q29 duplications. Chromosome 3 and corresponding genes are shown based on data from DECIPHER (https://decipher.sanger.ac.uk/). Horizontal thick bars indicate duplicated regions of the current patient and other registered patients. Green bars show epilepsy and blue bars show no epilepsy. From the top of the bars to the bottom, duplications are shown of the current case, 331860 (DECIPHER ID), 266509 (DECIPHER ID), each patient described by Lisi et al, Fernandez-Haen et al., Quintela et al., and patients 1 and 2 by Tassano et al. [19, 20, 25, 31]

Acknowledgements This work was supported by AMED under the grant numbers JP18ek0109280, JP18dm0107090, JP18ek0109301, JP18ek0109348, and JP18kk020501; JSPS KAKENHI grant numbers JP17H01539, JP16H05160, JP16H05357, JP16H06254, JP17K10080, JP 17K15630, and JP17H06994; the Takeda Science Foundation; and the Ichiro Kanehara Foundation for the Promotion of Medical Science and Medical Care. We also thank N. Watanabe, T. Miyama, M. Sato, and K. Takabe for their technical assistance. We would like to thank Editage (www.editage.jp) for English language editing. We thank all patients and their families for their participation in this study.

Compliance with ethical standards

Conflict of interest The authors declare that they have no conflict of interest.

Publisher's note: Springer Nature remains neutral with regard to jurisdictional claims in published maps and institutional affiliations.

References

1. Goldfarb M. Voltage-gated sodium channel-associated proteins and alternative mechanisms of inactivation and block. Cell Mol Life Sci. 2012;69:1067–76.
2. Siekierska A, Isrie M, Liu Y, Scheldeman C, Vanthillo N, Lagae L, et al. Gain-of-function FHF1 mutation causes early-onset epileptic encephalopathy with cerebellar atrophy. Neurology. 2016;86:2162–70.
3. Al-Mehmadi S, Splitt M, Ramesh V, DeBrosse S, Dessoffy K, Xia F, et al. FHF1 (FGF12) epileptic encephalopathy. Neurol Genet. 2016;2:e115.
4. Guella I, Huh L, McKenzie MB, Toyota EB, Bebin EM, Thompson ML, et al. De novo FGF12 mutation in 2 patients with neonatal-onset epilepsy. Neurol Genet. 2016;2:e120.
5. Villeneuve N, Abidi A, Cacciagli P, Mignon-Ravix C, Chabrol B, Villard L, et al. Heterogeneity of FHF1 related phenotype: Novel case with early onset severe attacks of apnea, partial mitochondrial respiratory chain complex II deficiency, neonatal onset seizures without neurodegeneration. Eur J Paediatr Neurol. 2017; 21:783–86.
6. Takeguchi R, Haginoya K, Uchiyama Y, Fujita A, Nagura M, Takeshita E, et al. Two Japanese cases of epileptic encephalopathy associated with an FGF12 mutation. Brain Dev. 2018;40:728–32.
7. Iwama K, Sasaki M, Hirabayashi S, Ohba C, Iwabuchi E, Miyatake S, et al. Milder progressive cerebellar atrophy caused by biallelic SEPSECS mutations. J Hum Genet. 2016;61:527–31.
8. Saitsu H, Nishimura T, Muramatsu K, Kodera H, Kumada S, Sugai K, et al. De novo mutations in the autophagy gene WDR45 cause static encephalopathy of childhood with neurodegeneration in adulthood. Nat Genet. 2013;45:445–9, 49e1.
9. Higasa K, Miyake N, Yoshimura J, Okamura K, Niihori T, Saitsu H, et al. Human genetic variation database, a reference database of genetic variations in the Japanese population. J Hum Genet. 2016;61:547–53.
10. Miyatake S, Koshimizu E, Fujita A, Fukai R, Imagawa E, Ohba C, et al. Detecting copy-number variations in whole-exome sequencing data using the eXome Hidden Markov Model: an 'exome-first' approach. J Hum Genet. 2015;60:175–82.
11. Tsuchida N, Nakashima M, Kato M, Heyman E, Inui T, Haginoya K, et al. Detection of copy number variations in epilepsy using exome data. Clin Genet. 2018;93:577–87.
12. Nord AS, Lee M, King MC, Walsh T. Accurate and exact CNV identification from targeted high-throughput sequence data. BMC Genom. 2011;12:184.
13. Fromer M, Moran JL, Chambert K, Banks E, Bergen SE, Ruderfer DM, et al. Discovery and statistical genotyping of copy-number variation from whole-exome sequencing depth. Am J Hum Genet. 2012;91:597–607.
14. Fujita A, Suzumura H, Nakashima M, Tsurusaki Y, Saitsu H, Harada N, et al. A unique case of de novo 5q33.3-q34 triplication with uniparental isodisomy of 5q34-qter. Am J Med Genet A. 2013;161a:1904–9.
15. Miyake N, Abdel-Salam G, Yamagata T, Eid MM, Osaka H, Okamoto N, et al. Clinical features of SMARCA2 duplication overlap with Coffin-Siris syndrome. Am J Med Genet A. 2016;170:2662–70.
16. Mikati MA, Kurdi R, El-Khoury Z, Rahi A, Raad W. Intravenous immunoglobulin therapy in intractable childhood epilepsy: open-label study and review of the literature. Epilepsy Behav. 2010;17:90–4.
17. Ballif BC, Theisen A, Coppinger J, Gowans GC, Hersh JH, Madan-Khetarpal S, et al. Expanding the clinical phenotype of the 3q29 microdeletion syndrome and characterization of the reciprocal microduplication. Mol Cytogenet. 2008;1:8.
18. Goobie S, Knijnenburg J, Fitzpatrick D, Sharkey FH, Lionel AC, Marshall CR, et al. Molecular and clinical characterization of de novo and familial cases with microduplication 3q29: guidelines for copy number variation case reporting. Cytogenet Genome Res. 2008;123:65–78.
19. Fernandez-Jaen A, Castellanos Mdel C, Fernandez-Perrone AL, Fernandez-Mayoralas DM, de la Vega AG, Calleja-Perez B, et al. Cerebral palsy, epilepsy, and severe intellectual disability in a patient with 3q29 microduplication syndrome. Am J Med Genet A. 2014;164a:2043–7.
20. Tassano E, Uccella S, Giacomini T, Severino M, Siri L, Gherzi M, et al. 3q29 microduplication syndrome: Description of two new cases and delineation of the minimal critical region. Eur J Med Genet. 2018;61:428–33.
21. Swinkels ME, Simons A, Smeets DF, Vissers LE, Veltman JA, Pfundt R, et al. Clinical and cytogenetic characterization of 13 Dutch patients with deletion 9p syndrome: Delineation of the critical region for a consensus phenotype. Am J Med Genet A. 2008;146a:1430–8.
22. Hulick PJ, Noonan KM, Kulkarni S, Donovan DJ, Listewnik M, Ihm C, et al. Cytogenetic and array-CGH characterization of a complex de novo rearrangement involving duplication and deletion of 9p and clinical findings in a 4-month-old female. Cytogenet Genome Res. 2009;126:305–12.
23. Recalcati MP, Bellini M, Norsa L, Ballarati L, Caselli R, Russo S, et al. Complex rearrangement involving 9p deletion and duplication in a syndromic patient: genotype/phenotype correlation and review of the literature. Gene. 2012;502:40–5.
24. Kawara H, Yamamoto T, Harada N, Yoshiura K, Niikawa N, Nishimura A, et al. Narrowing candidate region for monosomy 9p syndrome to a 4.7-Mb segment at 9p22.2-p23. Am J Med Genet A. 2006;140:373–7.
25. Lisi EC, Hamosh A, Doheny KF, Squibb E, Jackson B, Galczynski R, et al. 3q29 interstitial microduplication: a new syndrome in a three-generation family. Am J Med Genet A. 2008;146a:601–9.
26. Hamdan FF, Myers CT, Cossette P, Lemay P, Spiegelman D, Laporte AD, et al. High rate of recurrent de novo mutations in developmental and epileptic encephalopathies. Am J Hum Genet. 2017;101:664–85.
27. Bowling KM, Thompson ML, Amaral MD, Finnila CR, Hiatt SM, Engel KL, et al. Genomic diagnosis for children with intellectual disability and/or developmental delay. Genome Med. 2017;9:43.
28. Szinnai G. Clinical genetics of congenital hypothyroidism. Endocr Dev. 2014;26:60–78.

29. Gunes S, Ekinci O, Ekinci N, Toros F. Coexistence of 9p deletion syndrome and autism spectrum disorder. J Autism Dev Disord. 2017;47:520–21.
30. Kowalewski AM, Szylberg L, Kasperska A, Marszalek A. The diagnosis and management of congenital and adult-onset hyperinsulinism (nesidioblastosis)-literature review. Pol J Pathol. 2017;68:97–101.
31. Quintela I, Barros-Angueira F, Perez-Gay L, Dacruz D, Castro-Gago M, Carracedo A, et al. Molecular characterisation and phenotypic description of two patients with reciprocal chromosomal aberrations in the region of the 3q29 microdeletion/microduplication syndromes. Rev Neurol. 2015;61:255–60.